

## Surface Characteristics Analysis and Adherence Evaluation of Hot-Dip Galvanized Low Alloy Steel

### Analyse des caractéristiques de surface et évaluation de l'adhérence d'un acier à bas carbone galvanisé à chaud

Lamia Darsouni<sup>\*1</sup>, Mohamed Zine Touhami<sup>1</sup>, Abdelkader Khettache<sup>2</sup> & Omar Benchiheb<sup>1</sup>

<sup>1</sup>Foundry Laboratory, Department of Metallurgy, Badji-Mokhtar University, PO Box 12, 23000, Annaba, Algeria.

<sup>2</sup>Laboratory of Physical Metallurgy and Mechanical Properties, Department of Metallurgy, Badji-Mokhtar University, PO Box 12, 23000, Annaba, Algeria.

Soumis le : 02/10/2017

Révisé le : 26/02/2018

Accepté le : 01/03/2018

#### ملخص

تتناول هذه الدراسة تحليل السمات السطحية و تقييم التصاق طلاء- الركيزة لعينات من ألواح الصلب المجلفن بالغمس الساخن التي ينتجها مصنع أرسيلور ميتال. كشف المجهر الضوئي أن الطلاء مشكل أساسا من أكسيد الزنك، طبقة الزنك النقي ( $\eta$ )، طبقة السبائك زيتا ( $\zeta$ )، الطبقة دلتا ( $\delta$ ) وطبقة التثبيط  $\Gamma$ . دراسة التفاعل الركيزة وطلاء بواسطة المجهر الإلكتروني و(EDX) أظهرت وجود كمية كبيرة من الأكسجين مركزة في الواجهة على شكل أكسيد الحديد حيث تمنع انتشار الزنك وبالتالي تقليل التصاق الطلاء على الركيزة. يرتبط أيضا التصاق الضعيف بوجود طبقة السبائك التي هي هشنة بطبيعتها. اختبار المسافة البادئة البينية يستعمل لتحديد صلابة كسر المسافة البادئة بين الطلاء حديد- زنك. أثناء الاختبار، بدأت الشقوق تظهر وتنتشر على طول الواجهة. وقد تبين أن الشقوق من الشكل tsivqmlaP تظهر ابتداءا من N0,5 والمعامل  $K_{IC}$  ينخفض مع الزيادة في الحمل الطبيعي. اختبارين التآكل الكهروكيميائية أظهرت أن جميع الطلاء لديها مقاومة التآكل أعلى بكثير من الصلب غير المصقول.

**الكلمات المفتاحية:** سبائك الصلب المنخفض- المجلفن بالغمس الساخن- الطلاء - المسافة البادئة البينية- الصلابة.

#### Abstract

The present study discusses the surface characteristics analysis and coating - substrate adherence evaluation of samples from hot-dip galvanized steel sheets produced by Arcelor Mittal Company. Optical microscopy has revealed that the coating is formed principally of zinc oxide (ZnO), pure zinc ( $\eta$ ) layer, intermetallic phase zeta ( $\zeta$ ), the existence of Delta ( $\delta$ ) phase, and  $\Gamma$ -inhibition layer. The Scanning Electron microscopy with EDX studies on substrate-interface and coating showed the presence of oxygen in large quantities localized in the interface and which is the formation of iron oxides that prevent the diffusion of zinc and therefore reduces the adhesion of the coating to the substrate. The low adhesion is also related to the presence of intermetallic phases which are inherently fragile. The interfacial indentation test allows determining the indentation fracture toughness of Fe-Zn coatings. During the test, a crack is initiated and propagated along the interface. It was demonstrated that cracks Palmqvist type appear from 0.5N and the  $K_{IC}$  coefficient decreases according to the increase of the normal load. The contaminations of samples coated before and after ion sputtering were analyzed using X-ray Photoelectron Spectroscopy (XPS). Both electrochemical corrosion tests in a 3.5% NaCl solution showed that all Fe-Zn coatings have a much higher corrosion resistance than that for steel uncoated.

**Keywords:** Low alloy steel - Continuous hot-dip galvanizing - Coatings - Interfacial Indentation - tenacity.

#### Résumé

La présente étude traite l'analyse des caractéristiques de surface et de l'évaluation de l'adhérence revêtement-substrat d'échantillons des tôles d'acier galvanisé à chaud produites par l'usine de Arcelor Mittal. La microscopie optique a révélé que le revêtement est formé principalement d'oxyde de zinc (ZnO), de couche de zinc pur ( $\eta$ ), d'intermétallique phase zéta ( $\zeta$ ), de la phase Delta ( $\delta$ ) et de couche d'inhibition  $\Gamma$ . L'étude de l'interface et du revêtement du substrat par microscopie électronique à balayage et EDX a montré la présence d'une grande quantité d'oxygène localisée dans l'interface sous forme d'oxydes de fer qui empêchent la diffusion du zinc et réduit ainsi l'adhérence du revêtement sur le substrat. La faible adhérence est également liée à la présence des phases intermétalliques qui sont intrinsèquement fragiles. Le test d'indentation interfaciale permet de déterminer la ténacité de rupture de l'indentation des revêtements Fe-Zn. Au cours du test, des fissures sont initiées puis propagées le long de l'interface. Il a été démontré que les fissures du type Palmqvist apparaissent à partir de 0,5N et que le coefficient de  $K_{IC}$  diminue en fonction de l'augmentation de la charge normale. Les deux tests de corrosion électrochimiques réalisés dans une solution de NaCl à 3,5% ont montré que tous les revêtements Fe-Zn présentent une résistance à la corrosion beaucoup plus élevée que celle de l'acier non revêtu.

**Mots clés:** Acier faiblement allié - Galvanisation à chaud - Revêtements - Indentation interfaciale- Ténacité.

\* Auteur correspondant: ch-lamia@hotmail.fr

## 1. INTRODUCTION

Hot dip galvanizing using zinc and zinc alloy coatings is one of the most commercially important and oldest methods to protect steel from corrosive media. Hot dip galvanizing is the process of coating iron or steel with a zinc layer, by passing the steel through a molten bath of zinc at a temperature of around 460°C [1]. Hot-dip galvanized steel is now being used in more demanding applications such as automotive body panels, where any tiny blemish on the coating is objectionable for the exposed surface [2,3].

The most common commercial processing technique used to protect steel components in corrosive environments is hot-dip galvanizing with various applications in iron and steel components [4,5]. Fe-Zn layers of low alloy steels exhibits a variety of excellent mechanical properties, such as strength, toughness and ductility [6]. Steel is also easily manufactured and presents good formability, weldability and paintability [7]. Other positive factors include its availability, ferromagnetic properties, recyclability and low cost. Because steel is susceptible to corrosion in the presence of moisture and to oxidation at elevated temperatures, successful use of these favorable characteristics generally requires some form of protection [8]. Such defects damage the surface quality, leading to down grading the product where high surface quality is required. Zinc coatings produced by hot dip galvanizing is a multi-component system consisting of several phases, such as hexagonal zinc,  $\Gamma$ -Fe<sub>2</sub>Al<sub>5</sub> and  $\zeta$ -FeZn<sub>13</sub> [9], which make analysis of the coating/substrate system difficult. Moreover, detailed knowledge about the mechanical properties of these individual phases, as well as their interfacial properties, is lacking.

The strips produced by continuous hot-dip galvanizing line at the Arcelor Mittal company show poor adhesion of the Fe-Zn layers on A9 steel. The delaminating of these layers was observed during bending test. This delaminating of material is only the consequence of the microcracks initiation causing the poor adhesion which is not known to be in the coating-substrate-interface or in Fe-Zn layers. This localized defect in the material which is rejected induces a loss of material, and consequently a consumption of zinc and systematically a stoppage of work, resulting in a decrease in the production of the galvanized strips.

The parameters which can influence the adhesion are multiple, in particular the roughness induced by the cold rolling, the surface cohesion and the wettability [10]. However, cleaning as well as deposit characteristics such as phase composition, immersion time, coating thickness are decisive parameters. It is known that the thickness of continuous hot dip galvanized coating is essentially a function of the following parameters: The extraction rate of the sheet after immersion in bath zinc, temperature of the molten zinc, the angle or position of extraction of the sample, cooling of the galvanized product, internal stresses and cracks may occur in the layers and may result in a bond breaking and consequent the coating.

To provide an answer to these problems, it is necessary to employ characterization techniques that are very appropriate for surface problems such as optical microscopy, scanning electron microscopy with energy dispersive spectrometry (EDS), XPS spectroscopy, X-ray diffraction, adherence tests using interfacial indentation, corrosion tests, as well as linear profilometry 2D.

## 2. EXPERIMENTAL PROCEDURE

Samples from hot-dip galvanized steel sheets produced by Arcelor Mittal Steel Company were used for this investigation. The manufacturing conditions including hot and cold rolling, annealing process and hot dip galvanizing were the same for all sheets used in this study. The investigated material was industrially produced dual phase steel (designated as A9) with the chemical composition: Fe(bal.) - 0.06C- 0.45Mn-0.04Si-0.05Al- 0.02P-0.02S (in wt. %). Steel was supplied in the form of 0.38mm, 0.9mm and 1.9mm thick cold rolled sheets. The parameters of annealing and coatings processes are shown in Table 1. The molten zinc bath contained 0.50 wt. %Al and 0.30wt. %Pb. The chemical composition of the zinc bath was in the same range for all specimens. Prior to immersion in liquid zinc at 460°C for 4s, the steel sheet was annealed in the intercritical temperature range 700-800°C to produce a DP microstructure, ferrite and austenite [11]. When the steel sheet was removed from the liquid zinc bath it was immediately cooled down to room temperature in a stream of N<sub>2</sub> gas. Cross sections of the substrates coated were prepared by conventional metallography method and examined by optical microscopy. The specimens were etched in a 3% solution of nital, to observe the surface morphologies of layers, using BX51M Olympus microscope and a Scanning Electron

Microscope Zeiss Ultra TM55 type and the compositions of substrate-interface-coatings were determined using energy dispersive spectroscopy (EDS) analysis.

The interfacial indentation test allows determining the indentation fracture toughness of Fe-Zn coatings. During the test, a Vickers indentation (Fig.1) is carried out on cross section of the sample. In order to determine the Vickers microhardness indenter Shimadzu HMV-2000 with loads of 0.25, 0.5, 1.00, 2.00, 5.00, 10.00 and 20N were used. Among the models existing and allowing calculating the fracture toughness ( $K_{Ic}$ ) of Fe-Zn coating on the substrate, we have chosen the corresponding to traditional Palmqvist crack model [10].

$$kc = 0,0319 \frac{P}{a l^{1/2}} \quad (\text{Eq.1})$$

where P (applied load),  $c = l + a$ ,  $l$  (crack length generated at the edges of the indentation marks at the maximum applied load),  $a$  – half diagonal-length of the indentation mark [10].

X-ray diffraction (XRD) patterns of the different layers were determined by means of Bruker D8 Advance Model diffractometer with a  $\text{CuK}\alpha$  radiation with a wavelength of  $1.5406\text{\AA}$ .

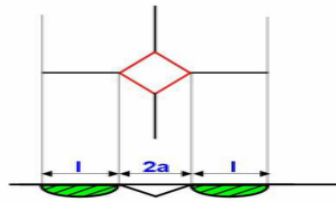


Figure1. Crack Palmqvist type formed during Vickers test [12].

Measurements were performed by applying 45kV voltages and 35mA current Polarization tests were performed to further investigate the corrosion behavior. The test was conducted in a 3.5% NaCl solution at room temperature using a Gamry model 600 associated with a Gamry Framework software 2273 electrochemical system. A standard corrosion cell kit with a working electrode, two graphite counter electrodes, and an Ag/AgCl reference electrode were used. Potentiodynamic scanning was performed by stepping the potential at a scan rate of 1 mV/s from -150 to +200 mV.

Table 1. Technological parameters of recrystallization annealing and hot-dip galvanizing

<b>Thickness of sheets (mm)</b>	0,38	0,9	1,9
<b>Roughness (<math>R_a</math>) before galvanizing process (<math>\mu\text{m}</math>)</b>	0,42	0,29	0,44
<b>Defilement speed of sheet (m/min)</b>		32-150	
<b>Furnace atmosphere used</b>		$\text{HN}_x$	
<b>Temperature of recrystallization annealing (<math>^{\circ}\text{C}</math>)</b>		700-800	
<b>Chemical Composition of the bath in wt. %</b>	Zn (99.00%)	Al (0.5%)	Pb (0.3%)
<b>Zinc bath temperature (<math>^{\circ}\text{C}</math>)</b>		460	
<b>Immersion time (s)</b>		04	
<b>Surface roughness after immersion</b>	0,27	0,51	0,69

The exposed area was  $1.0\text{cm}^2$  in all specimens selected for polarization tests. A standard corrosion cell kit with a working electrode, two graphite counter electrodes, and an Ag/AgCl reference electrode were used.

The XPS analysis of the top surface concentrations and the bonding state of the elements were performed in a PH Quantum 2000 XPS spectrometer. Contaminations and oxide layer thickness was defined using the XPS depth profiles which were recorded with a sputter rate of 15nm/min.

### 3. RESULTS AND DISCUSSION

#### 3.1. Microstructures of the substrate/coating surface

Figure.2 shows the microstructure of steel A9 intended for galvanizing. It is formed mainly of ferrite and pearlite grains.

However, the annealing of the cold-rolled sheets produced in the temperature range 700-800°C caused in certain ranges, elongated ferrite and pearlite grains and in others some grains not recrystallized. The non-completion of the recrystallization of grains is due to our opinion to the inadequate annealing time of the sheet. Figures.3 (a, b, c) shows the flowering, appearance of the zinc crystals. Macrographics observations made on the surfaces of the samples having undergone galvanization show a regular flowering in the size of the crystals varies from one coating to another. This flowering (appearance of the zinc crystals) is observed in all the samples of different thicknesses. Referring to the X-ray diffraction results (Figs.6a-c), it has been found that despite different thicknesses of the coatings; we have the formation of the same phases. From these results, we can conclude that the steel surface roughness doesn't influence the phases of the zinc coating, but has influence on the thickness. The relief of the steel substrate influences on Fe-Zn alloy coatings [14], when the relief of the steels substrate is rough, that crystallites grow elongated and when the relief is smooth, the crystallites grows rounded [14]. This case is observed for the sample of 1.9mm thickness and a roughness (Ra) is 0.44 $\mu\text{m}$  (Fig.3C).

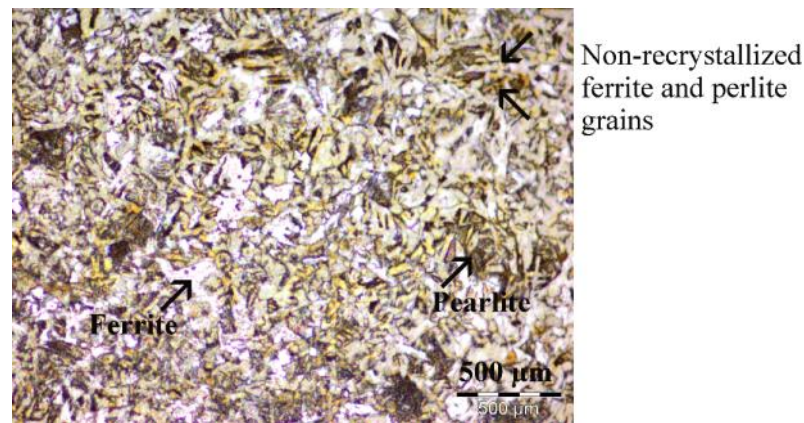


Figure 2. Optical micrographs showing the microstructure of A9 steel substrate.

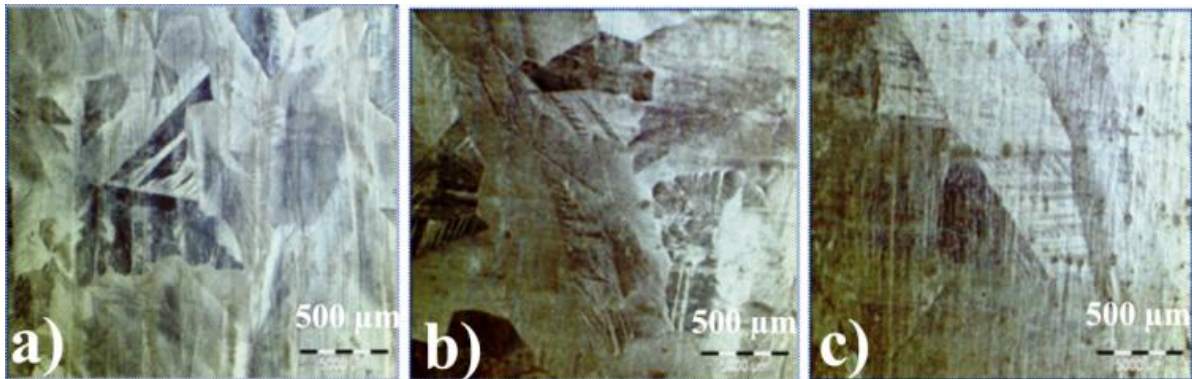


Figure 3 (a,b,c). Superficial aspect of steels galvanized  
Thickness of sheet: a) 0.38mm,b) 0.90mm,c) 1.90mm.

### 3.2. Microstructure of coatings/substrate

The coating microstructure of a sample galvanized for 4s is shown in Fig.5. It was found for all specimens hot dip galvanized have the same phases confirmed by X-ray diffraction analysis Figs.4 and 6 such as  $\Gamma$ -  $\text{Fe}_2\text{Al}_5$  ( $\text{Fe}_2\text{Al}_5\text{-Zn}_x$ ), and  $\text{Fe}_{11}\text{Zn}_{40}$  phases next to the steel substrate, and  $\text{FeAl}_3$  ( $\text{FeAl}_3\text{-Zn}_x$ ) phase next to coating surface [15]. In reality, the reactions occurring in a galvanizing system and mechanisms controlling the nucleation and growth of Fe-Zn intermetallic phases are very complex due to the addition of different elements mostly Al into the Zn bath (0.5 wt.%), impurities in the ferrous substrate, coincidence of different reactions at the interface, their fast kinetics and non-equilibrium conditions governing the process [17].

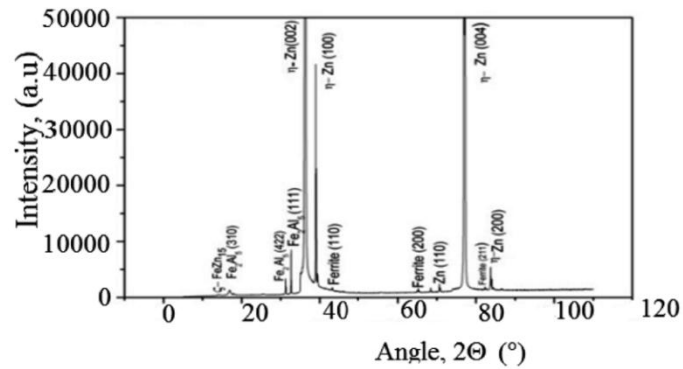


Figure 4. X-ray diffraction spectrum of A9 steel hot-dip galvanized

a) Grazing angle diffraction ( $\omega=1^\circ$ ). In our case, the introduction of low Al content (0.5 wt%) added to the Zn bath prevent the formation of the Fe-Zn intermetallic phases by the formation of an inhibition layer [16]. The minimum amount of Al needed for the full inhibition is around 0.15 wt% at 450°C [16]. According to the Tang N.Y. [18] study, the inhibition layers form in two steps involving (a) an Al uptake and subsequent nucleation of  $\text{Fe}_2\text{Al}_5\text{Zn}_x$  layer at the substrate interface, and (b) the growth of the inhibition layer by the diffusion of Zn atoms across the layer. The  $\text{Fe}_2\text{Al}_5\text{Zn}_x$  inhibition layer has a fine granular structure and an orthorhombic structure with around 23 wt% Zn [16]. The intermetallic phases constituted by one layer called inhibition layer is very thin (from 50 to 150nm) is characterized by a hardness and non acceptable toughness [19]. The inhibition layer will be thin and, consequently, more iron (Fe) will diffuse into the liquid zinc to form Fe-Zn compounds.

The impact of pre-oxidation on surface subsurface and coating of steel containing C (0.16 wt %), Mn (1.6 wt %), Si (1.5 wt %), Al (<0.05 wt %) has been investigated by Martin Norden et al. [20]. They found that Mn-Si oxides lead to deterioration in zinc wetting, and bare spots can emerge. Furthermore, zinc adhesion diminishes, as the  $\text{Fe}_2\text{Al}_5$  inhibition layer formation is hampered by these Mn-Si oxides.

The upper layer of so called  $\eta$ -phase is consisting practically of the pure zinc and is formed by simple solidification of the zinc melt. From the metallurgic aspect, however, this phase is defined as a solid substitutional solution of iron in the zinc (content of the iron is about 0.03 wt. %).

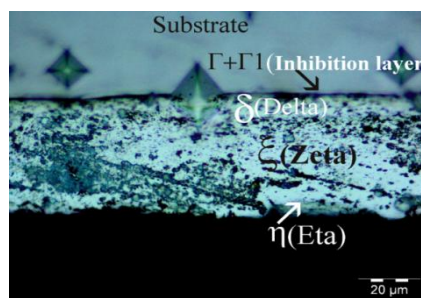


Figure 5. Optical micrograph from cross section of hot dip galvanized steel with different layers of the coating. Thickness of sheet (2mm).

Zinc crystallizes in the hexagonal system (hcp) and is characterized in relatively high toughness under common temperatures and low hardness [21].

X-ray diffraction results show (Fig.4) using glancing angle diffraction ( $\omega = 1^\circ$ ), the presence of interface layer ( $\Gamma$ -  $\text{Fe}_2\text{Al}_5$ ) between substrate and zinc coating. Other hand, it is constated also, for a small glancing angle diffraction ( $\omega=0.001^\circ$ ) for all samples with different thickness (Fig.6a-c), the formation in contact directly to substrate, the same phase  $\Gamma$ - $\text{Fe}_2\text{Al}_5$ .

It is well known that the formation of  $\Gamma$  phase is prevented effectively by addition of a small amount of aluminum, normally less than 1%, in the melt. In the presence of aluminum, steel reacts preferentially with aluminum to form a thin, continuous layer of  $\text{Fe}_2\text{Al}_5$  at the melt/steel interface.



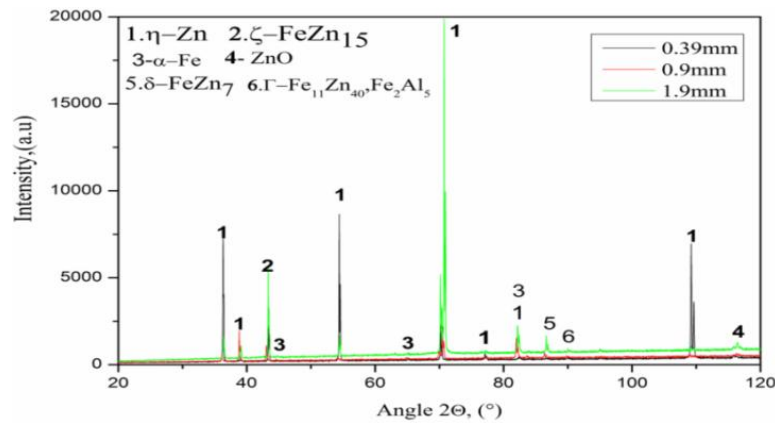


Figure 6. X- ray diffraction spectrum of A9 steel hot- dip galvanized  
b) Grazing angle diffraction ( $\omega=0.001^\circ$ ),

Direct contact between zinc melt and steel is now avoided and the growth of  $\Gamma$  phase is prevented. Others layers appeared such as  $\delta$ -FeZn<sub>7</sub>,  $\zeta$ -FeZn<sub>15</sub>,  $\eta$ -Zn and ZnO in extremely surface. These compounds, usually  $\zeta$ -FeZn<sub>15</sub>, nucleate on top of the inhibition layer. Hence, Fe diffuses from the steel substrate into the zinc bath through the solid inhibition layer.

### 3.3. Adherence evaluation

The thickness of coatings varies from 5 to 15 $\mu$ m, when the thickness of sheet passes from 0.38mm to 1.9mm. This difference is explained probably by a roughness surface effect. The optical microscopy observations on cross sections of samples showed the Fe-Zn coatings (Figs.7a-c). The thickness of these layers varies from 5 to 15 $\mu$ m when the thickness changes from 0.38 to 1.9mm. It was noted that the mechanical polishing on the galvanized samples resulted a delaminating for thick layers. However; we have recorded for the layers of small thicknesses a good adhesion (Fig.7a). The presence of the oxide layers formed during recrystallization annealing; residual deposits from the pickling process and cold rolling significantly impeded the zinc diffusion and the formation of the first bonding interface. C.E. Jordan and al [22] have studied the effect of Iron Oxide as an inhibition layer on Iron-Zinc. They have founded, in a pure Zn bath, the oxide present on the surface of low-carbon steel substrate acts as a physical barrier that inhibits Fe and Zn reactions at short immersion times.

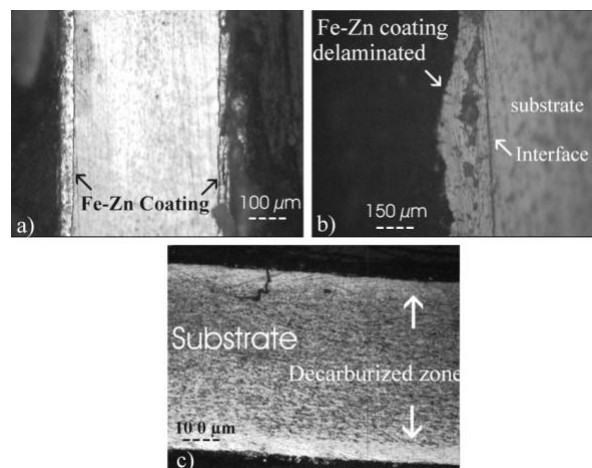


Figure 7 (a,b,c). Optical micrographs of cross section samples hot dip galvanized  
a, b) thickness of sheets 0.38mm and 1.9mm  
c) sample galvanized showing the decarburizing zone.

By observing the appearance of the surfaces of the sheets galvanized, we can say that a ferritization occurred during recrystallization annealing carried out in an oxidizing and decarburizing atmosphere, despite the presence of  $\text{NH}_x$  gas (Fig.7c). This is confirmed by microhardness tests which were carried out on a cross section of the sample 0.9mm of thick approximately from the surface and at the core  
©UBMA - 2018

and which gave respectively 160HV<sub>0.05</sub> and 250HV<sub>0.05</sub>. The value which is 160HV<sub>0.05</sub> corresponds to the hardness of the ferrite phase, and the value of 250HV<sub>0.05</sub> corresponds perfectly to the pearlitic constituent component which has poor adhesion to the galvanized layers. Referring to Fe-Zn equilibrium diagram [23], we can confirm that the high carbon concentration in the steel does not contribute to improving the adhesion of the Fe-Zinc layers. For this reason, galvanizing process is best applied for low carbon steels.

Ferritization as shown in the (Fig.7c) is very heterogeneous, it affects some lateral parts and others non-ferritized which means non-oxidized and decarburized which shows the presence of the pearlitic component (dark areas) and the solid solution α-Fe (light areas) caused by the oxidation and decarburization.

Ferritization phenomenon of the surfaces greatly improves the adhesion of Fe-Zinc layers to the steel substrate and mainly for the thin and medium plates. EDX analyzes on cross sections of the galvanized samples showed the presence of oxygen on the substrate-coating bond interface; which amply justifies the formation of a thin film of iron oxides which can play an important role in blocking the zinc diffusion on substrate (Figs.8a-c).

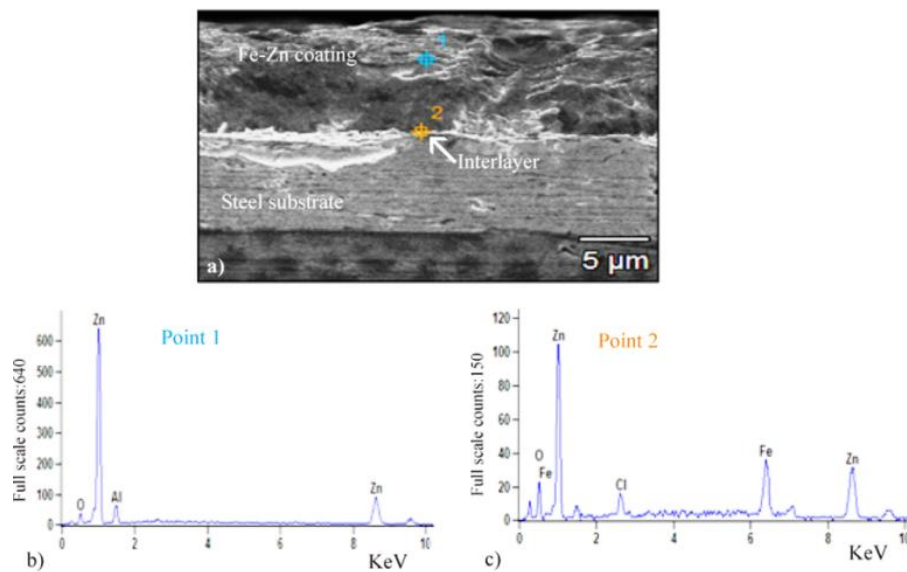


Figure. 8 (a,b,c). a) SEM micrograph b) and c) EDX analysis on cross section of A9 steel hot dip galvanized.

### 3.4. Indentation fracture toughness ( $K_{Ic}$ ) of hot dip galvanized steel

Observing the micrographs (Figs.9a-d), we see clearly that with the increase of the applied load; we obtain a systematic increase of the crack length which passes from 7.7μm for a load of 0.50N and 51.19μm for a load of 5N. Otherwise, crack initiation is achieved for a load of 0.5N. For loads in the range of 0.5N -1N, we observe a slight increase of the crack; on the other hand, beyond this load the crack becomes very important. To better elucidate this variation, we present the curve evolution the length crack versus applied load (Fig.10a). Referring to the literature; we were able to define the shape of the cracks caused by the Vickers test. We found that the type of cracks obtained corresponds to cracks of the Palmqvist type which states that in this model; the cracks propagate under the surface and only at the edges of the indentation and following the substrate-coating- interface [10].

Poton and Rawlings [13] refer to four models associated with Palmqvist cracking but in different forms depending on the ratio  $c/a$  or  $l/a$ . For  $l/a$  the ratio ranging from 0.25 to 2.5.

$$Kc = 0.0089 \left( \frac{E}{H} \right)^{\frac{2}{5}} \frac{P}{al^{1/2}} \quad (\text{Eq.1})$$

For ratios  $1 \leq l/a \leq 2.5$

$$Kc = 0.0122 \left( \frac{E}{HV} \right)^{\frac{2}{5}} \frac{P}{al^{1/2}} \quad (\text{Eq.2})$$

$$Kc = 0.0143 \left( \frac{E}{HV} \right)^{\frac{2}{5}} \frac{P}{c^{3/2}} al^{1/2} \quad (\text{Eq.3})$$

Among these models; three of them show the ratio between the Young's modulus and the hardness. A single model of the four presents the advantage of only involving the parameters deduced directly from the experiment.

$$Kc = 0.0319 \frac{P}{al^{1/2}} \quad (\text{Eq.4})$$

Where P (applied load),  $c = l + a$ ,  $l$  (crack length generated at the edges of the indentation marks at the maximum applied load),  $a$  (half diagonal-length of the indentation mark).

E-Young's modulus, HV- Hardness Vickers (Fig.10b) shows interfacial fracture toughness evaluated by Eq.4 as a function of applied load. It is clear that the indentation fracture toughness decreases with increasing the applied load. In the range of 0.5N to 2N, the indentation fracture toughness varies in the range between 0.35 to 0.26MPa.m<sup>1/2</sup>. The previous work carried out by Iost A. et al. [24] has found that the fracture toughness of the galvanized layers Fe-Zn is of the order 2MPa.m<sup>1/2</sup> using the same conditions, namely the interfacial indentation using the Vickers test under low loads and Palmqvist model.

This value corresponds to the indentation fracture toughness of the soft coatings. We attribute this low value to the poor adhesion of the Fe-Zn layers to the substrate. The weak adhesion is probably due to the effect of the layers of iron and aluminum oxides and the poor wettability of the liquid zinc which blocks the zinc diffusion [22].

Basically, the formation of the Fe-Al interfacial layer is very much hindered by the poor wettability of oxides that are formed on the surface during the annealing process [14] and this may cause the unwanted Fe-Zn outburst.

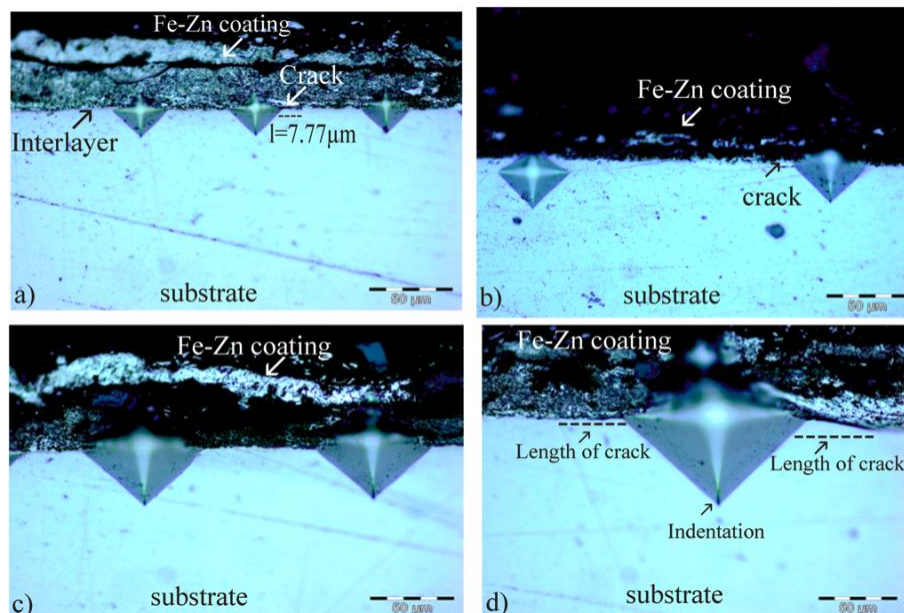


Figure 9 (a, b, c, d). Interfacial indentation on A9 steel hot dip galvanized using Vickers test under applied loads (sheet thickness 0.9mm). 0.50N, b) 1.00N, c) 2.00N, d) 5.00N



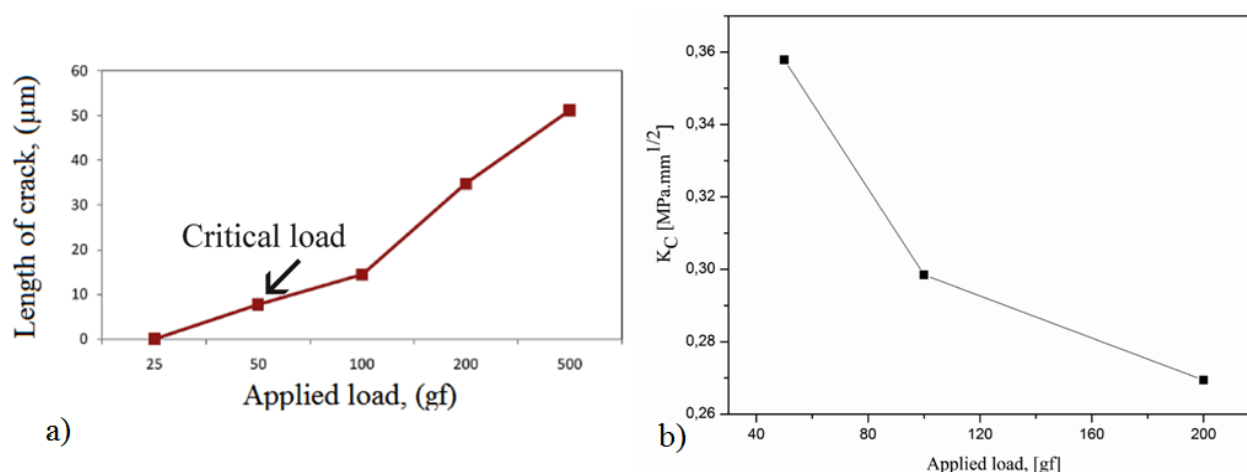


Figure. 10 (a, b). a) Schematic illustration of crack length ( $c$ ) and applied load ( $F$ )  
 b) Interfacial fracture toughness evaluated by Eq. 4 as a function of applied load.

Table 2. Indentation load effect on interfacial toughness fracture.

Indentation load (N)	Half indentation $a$ ( $\mu\text{m}$ )	Crack length $l$ ( $\mu\text{m}$ )	Interfacial toughness fracture $K_{Ic}$ ( $\text{MPa} \cdot \text{m}^{0.5}$ )
0.5	15,68	7,77	0,35786
1	27,62	14,40	0,29847
2	39,4	34,74	0,26942

### 3.5. XPS Analysis

XPS results show that the galvanized faces are contaminated; they contain organic material composed essentially of type phases.

These phases have a direct effect on the physicochemical properties of the material. We would like to point out that the ZnO phase has been formed called ( $\eta$ ) which overlaps with the oxygen in the air of a protective layer of Zinc Oxide (ZnO). This Zinc Oxide, formed directly after immersion, is transformed with moist air into zinc hydroxide  $\text{Zn}(\text{OH})_2$ .

The complementary action of the carbon dioxide ensures the formation of a very adherent insoluble ( $2\text{ZnCO}_3, 3\text{Zn}(\text{OH})_2$ ) hydroxycarbonate. These phases are presented by the XPS spectra (Fig. 11a).

Other complementary analyzes have been envisaged which involve etching the contamination of the galvanized surfaces by placing it in a reactor (Ion sputtering argon) or we have created a high vacuum and injected argon to remove all contamination. The sputtering speed is 15nm/min.

Figs. 11(b-f) show that the vacuum treatment and the injection of the argon made it possible to etch the substances deposited during the hot-dip galvanization process. The samples investigated by XPS show a significant contamination of the galvanized surfaces which are covered with carbon-based organic layers, low soda concentration, phosphates, layers of chromium oxides (high concentration) and Zinc (ZnO). It was also found Zinc and Aluminum Oxides ( $\text{AlOx}$ ).

The investigated samples show a significant contamination on the surface ( $C_c = 61.6$  at. % 90.5 at.-%). The surface of sample 1 (side A) is largely covered by carbon (organic layer). Soda (small concentration) is present on the surface of the samples A (side A and b). Phosphate can be detected too (sample 1, side A). Zinc phosphate is probably. Samples 1a and 1b show a small iron concentration on the surface. Otherwise it is typical for the samples 1a and 1b that chromium can be confirmed (high concentration). Zinc and aluminium were found after galvanization. The relevant compounds are ZnO and  $\text{AlOx}$  (that means not exactly  $\text{Al}_2\text{O}_3$ ).

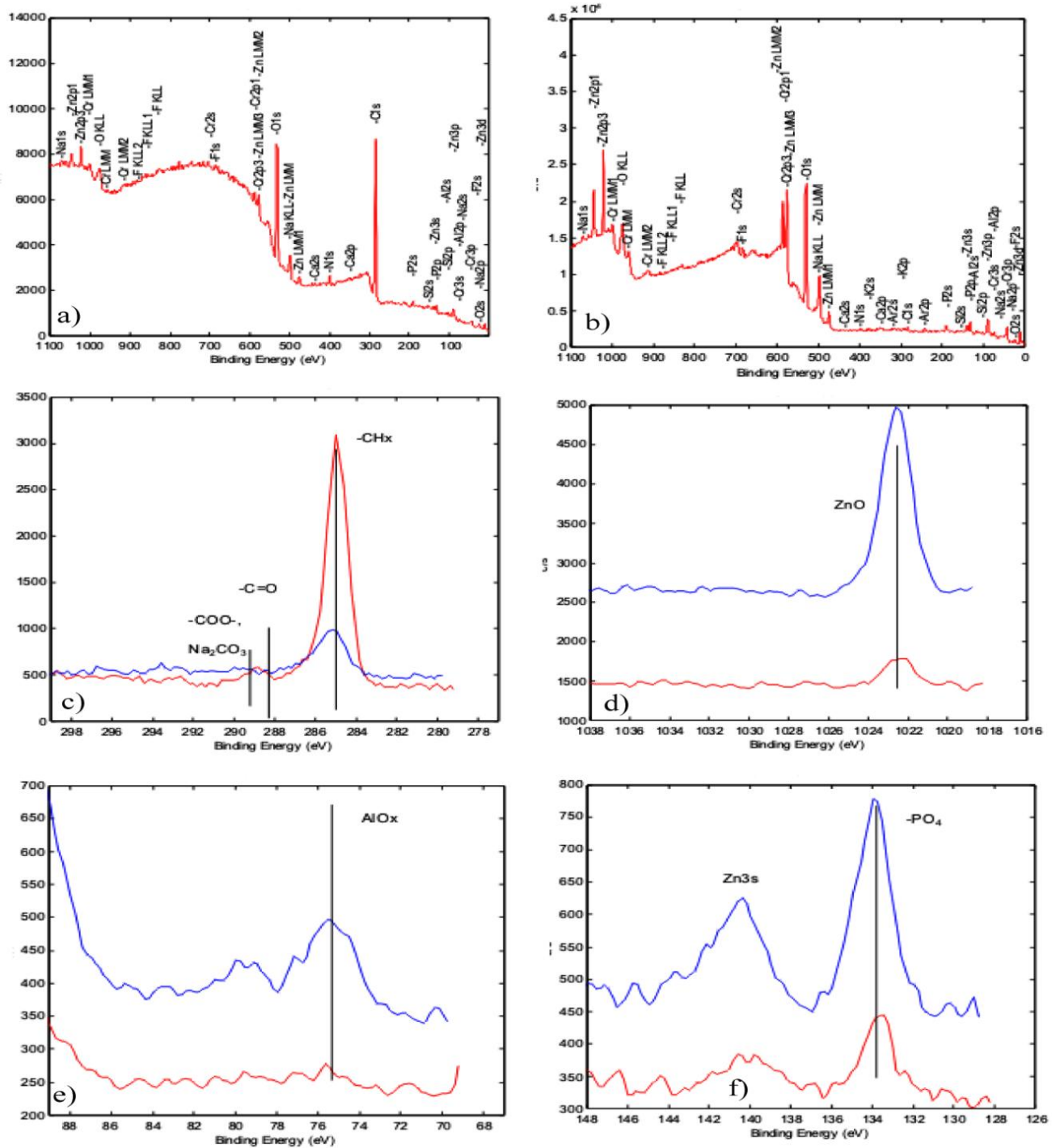


Figure. 11(a-f). XPS spectrum of A9 steel hot dip galvanized  
 a) sample coated , (b -f ) sample coated and cleaned with plasma argon.

### 3.6. Electrochemical behaviour

In some cases, the corrosion resistance of the galvanized layers is affected; this damage in relation to the raw state is probably related to the effect of the surface state, heterogeneity of the roughness, poor adhesion of the layers and other phenomena physico-chemical processes that require more exploration techniques. Some faces of the galvanized layers showed better corrosion behavior than the substrate. The performance of hot dip galvanized coating on steel not only depends on the alloy composition of the outer layer but also on the composition of the inner alloy layers of the coating substrate/interface [25]. It is important to mention that the presence of ZnO detected by X-ray diffraction in the case of thin and thick coatings therefore improves the corrosion resistance. (Figs.12(a, b)) shows the p

polarization curves between the two states and shows clearly the Fe-Zn coating on corrosion resistance. Table 3 summarizes all the corrosion properties of the various states.

Table 3. Corrosion parameters of A9 steel before and after hot- dip galvanized.

Corrosion parameters	Not coated	After coating
Corrosion rate (mpy)	3,797	2,029
Potential of corrosion $E(i=0)$ , (V)	-0,785	-1,118
Corrosion current density $i_{corr}$ ( $\mu\text{A}/\text{cm}^2$ )	29,13	15,65

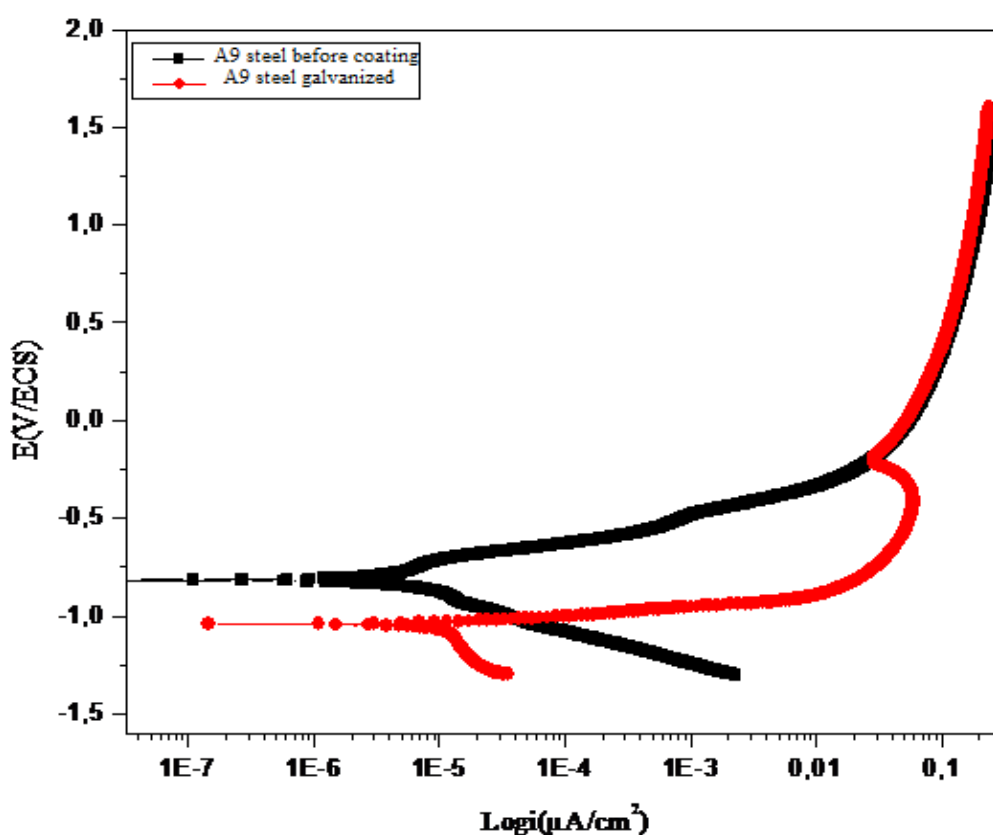


Figure 12. Tafel curves of A9 steel before and after hot dip galvanized

Figure.13 shows the evolution of the electrochemical impedance as a function of the frequency of the samples before and after galvanization. It has been found that for low frequencies, non-galvanized A9 steel has a high corrosion resistance characterized by the “Z” impedance, this increase being related to the surface state which is formed of highly resistant Iron Oxides corrosion and has good adhesion to the substrate. At high frequencies, we recorded a very significant decrease in impedance following the breakdown of the Iron Oxide film. For the Fe-Zn layers, it has been found that for low frequencies the impedance is low compared to the non-galvanized state, but at high impedances, the impedance decrease is less accentuated, probably due to the effect of the Fe-Zn layers which have better corrosion resistance and the destruction takes place progressively.

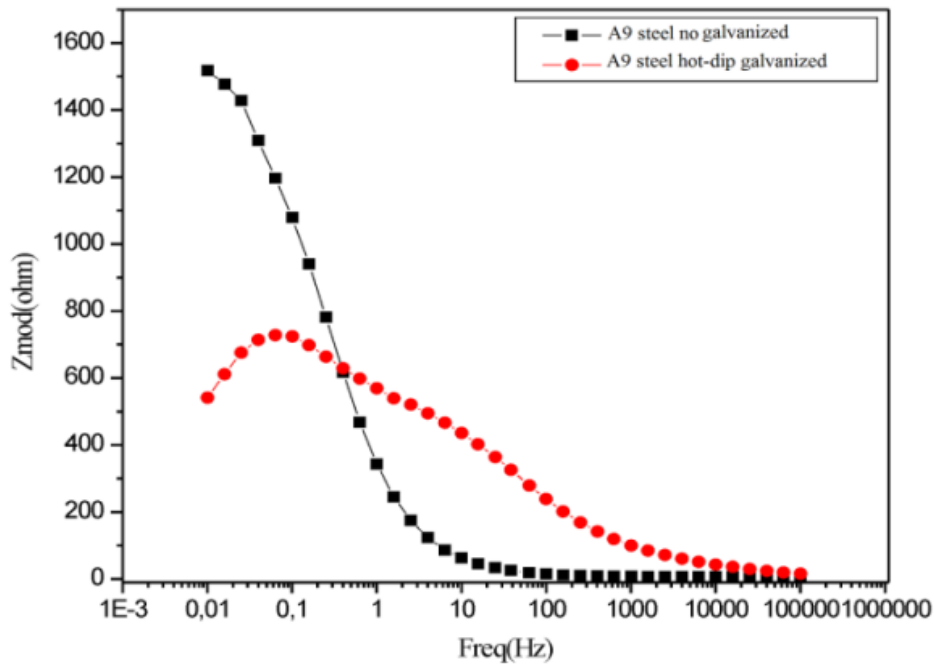


Figure 13. Variation of electrochemical impedance versus a frequency of A9 steels before coating and after hot-dip galvanized.

These results are confirmed by the Tafel curves (Fig.12a and Fig.12b) where they show that Fe-Zn layers have a better corrosion behavior compared to the non-galvanized state. Beyond the currents, the cathode branch is characterized by the formation of a stable bearing, which explains why there is formation of a passive film that is very corrosion resistant. Many works have showed than Fe-Zn layers are characterized by better corrosion resistance in media such as NaCl [26].

## CONCLUSION

The conclusions that can be drawn from this work are as follows:

The continuous hot-dip galvanizing line process applied to cold rolled and recrystallized sheets resulted in the formation of a compound layer such as  $ZnO$ ,  $\eta(Zn)$ ,  $\xi(FeZn_{15})$ ,  $\delta(FeZn_7)$  and inhibition layer  $\Gamma-(Fe_2Al_5-Zn_x, Fe_{11}Zn_{40})$ . The critical load which caused the separation between coating- substrate is 0.5N. Thus, the calculation of the indentation fracture toughness gave low values  $K_{Ic}$  ( $0.29-0.35 MPa.m^{0.5}$ ). The low adhesion of the coating to the substrate is due to the formation of the oxides formed during the recrystallization annealing and the contaminations which can generate the wettability. In a pure Zn bath, the oxide present on the surface of low-carbon steel substrate acts as a physical barrier that inhibits Fe and Zn reactions at short immersion times. Fe-Zn layers are characterized by better corrosion resistance in media (3.5% NaCl solution). From the XPS results, we have found that these galvanized layers are contaminated by organic substances that influence the corrosion behavior of these layers.

## REFERENCES

- [1] Abdel Hamid Z., Abdel Aal A., Hassan H.B. & Shaaban A., 2010. Applied Surface Science Process and performance of hot dip zinc coatings containing ZnO and Ni-P under layers as barrier protection *Applied Surface Science*, Vol. 256, 4166–4170.
- [2] Azimi., Ashrafizadeh F., Toroghinejad M.R. & Shahriari F., 2012. Metallurgical assessment of critical defects in continuous hot dip galvanized steel sheets, *Surface & Coatings Technology*, Vol. 206, 4376–4383A.
- [3] Ravi Shankar A., KamachiMudali U. & Raj B., 2009. *Eng. Fail. Anal.*, Vol. 16, 2485p.
- [4] Horstmann D., 1983. *Faults in Hot-dip Galvanizing*, second ed. G.m.b.H, Dusseldorf.
- [5] Vourlias G., Pistofidis N., Chaliampalias D., Patsalas P., Stergioudis G. & Tsipas D., 2006. E.K. Polychroniadis, *Surf. Coat. Technology*, Vol. 200, 6594.
- [6] Akoy, M.A., Kayali, E.S. & Cimenoglu H., 2004. The influence of microstructure features and mechanical properties on the cold formability of ferritic steel sheets, *ISIJ Int*, Vol. 44, 422-428.
- [7] Ravi Kumar D., 2002. Formability analysis of extra deep drawing steel, *Journal of Materials Processing Technology*, Vol. 130-131, 31-41.
- [8] Dafyidd H., Worsley D.A. & McMurray H.N., 2005. The kinetics and mechanism of cathodic oxygen reduction on Zinc and Zinc–Aluminium alloy galvanized coatings, *Corrosion Science*, Vol. 47, 3006-3018.
- [9] Gyurov S., Kostova Y. & Parshorov S., 2012. study on the possibility of Fe-Zn phase formation during hot-dipping in Zn 5% al melt at 450oc, *Journal of the University of Chemical Technology and Metallurgy*, Vol. 47 (2) , 211-216.
- [10] Etcheverry B., 6 December 2006. Adhesion, mechanics and tribology of multifunctional NiP - Talc composite coatings with reduced ecological footprint. Doctoral thesis in Science and materials engineering. The institut national polytechnique of Toulouse, France. p 126.
- [11] Szutkowska M., 2 October 2012. Fracture toughness of advanced alumina ceramics and alumina matrix composites used for cutting tool edges, *Journal of Achievement in Materials and Manufacturing Engineering*, Vol. 54, p 204.
- [12] Szutkowska M., 2005. Modified indentation methodes for fracture toughness determination of alumina ceramics. 13th International Scientific Conference on Achievements in Mecanical and materials engineering, Poland, 652.
- [13] Ponton C.B. & Rawlings R.D., 1989. Vickers indentation fracture toughness test. Part 1: Review of literature and formulation of standardised indentation toughness equations, *Materials Science Technology*, vol 5, 865-872.
- [14] Prabhudev S. & Swaminathan S., July 2011. Effect of oxides on the reaction kinetics during hot-dip galvanizing of high strength steels , *Corrosion Science*, Vol. 53, 2413 - 2418.
- [15] Gyurov S., Kostova Y. & Parshorov S., 2012. Study on the possibility of Fe-Zn phase formation during hot-dipping in Zn 5%al melt at 450OC S, *Journal of the University of Chemical Technology and Metallurgy*, Vol. 47(2), 211-216.
- [16] Marder A. R., 2000. *Progress in Materials. Science*. Vol 45, 191-271.
- [17] Guttman M., Lepretre Y., Aubry Y., Roche M.-J., Moreau T., Drillet P., Maigne J. M. & Baudin H., 1995. GALVATECH '95, *Iron and Steel Society*, Chicago, IL 295.
- [18] Tang N.-Y., Met., 1995. *Materials Transactions. A*, Vol 26, 1669-1704.
- [19] Elias J., Petit E., Lecomte J.S., Gay B. & Pitchon V., 2008. Tem study of the inhibition layer of commercial hot dip galvanized steels, *Materials Processing and texture. Ceramics Transactions*, A collection of papers Edited by A.D.Rollette presented at the 15<sup>th</sup> Inter.Conf. on textures of materials (ICOTOM15, Pittsburg, Pennsylvania Vol. 200.
- [20] Norden M., Blumenau M. & Schöenberg R., 2012. Recent Trends in Hot-Dip Galvanizing of Advanced High-Strength Steel at ThyssenKrupp Steel Europe, *Proceedings published by association Iron & Steel Technology, Conference AISTech, Atlanta 67-73*.
- [21] Mandal G.K., Mandal D., Das S.K., Balasubramaniam R. & S.P., 2009. Microstructural study of galvanized coatings formed in pure as well as commercial grade zinc baths Mehrotra, *Transactions of The Indian Institute of Metals*, Vol. 62, Issue 1, 35-40 TP 2252.
- [22] Jordan C.E. & Marder A.R., 1998. The Effect of Iron Oxide as an Inhibition Layer on Iron-Zinc Reactions during Hot-Dip Galvanizing, *Metallurgical and Materials Transactions B*, Vol. 29B, 479-484.
- [23] Pokorny P., Kolisko J., Balik L. & Novak P., 2015. Description of structure of Fe-Zn intermetallic compounds present in hot-dip galvanized, *Coatings on steel metalurgija*, Vol. 54 (4), 707-710.
- [24] IOST A. & FOCT J., 1993. Toughness and residual stresses in galvanizing, coatings *Journal of Materials Science letters*, Vol. 12, 1340-1343.
- [25] Abdel Z Hamid., Abdel A Aal., Hassan HB. & Shaaban A., 2010. Process and performance of hot dip zinc H.B coatings containing ZnO and Ni-P under layers as barrier, protection. *Applied Surface Science*, Vol. 256, 4166–4170.
- [26] SOUZA M.E.P, ARIZA E., BALLESTER M., ROCHA L.A. & FREIRE C.M. A., 2007. Comparative behaviour in terms of wear and corrosion resistance of galvanized and zinc-iron coated steels, *Revista Matéria*, Vol. 12 (4), 618 – 623.

## Acknowledgments

The authors thank “Arcelor Mittal Steel Company, Annaba, Algeria” for the samples given for experiment and galvanizing. Significant thanks to Pr. Xin Jiang and Petra from University of Siegen, Germany for interfacial Indentations and SEM images. Special thanks to The SGS Institute Fresenius, Germany for XPS analysis.